Influence of sample size on the onset temperature of yttria-stabilised zirconia flash sintering

João V. Campos[1*]; Isabela R. Lavagnini[1]; João G. Pereira da Silva[2]; Julieta A. Ferreira[1]; Rafael V. de Sousa[1]; Robert Mücke[2]; Olivier Guillon[2]; Eliria M. J. A. Pallone[1]
[1]Departamento de Engenharia de Biossistemas, Universidade de São Paulo, USP
AV. Duque de Caxias Norte, 225, Pirassununga-SP, Brazil.
[2]Forschungszentrum Jülich GmbH, Institute of Energy and Climate Research: Materials Synthesis and Processing (IEK-1), 52425 Jülich, Germany.
*Corresponding author e-mail address: joao2.campos@usp.br

Abstract

The influence of sample size on microstructure, density, and onset temperature of the flash event was investigated for 3 mol% yttria-stabilised zirconia. Pellet samples with different height and constant diameter were flash sintered under an AC electric field. The larger the samples were, the lower was their flash onset temperature. Furthermore, a more heterogeneous microstructure was verified on larger samples followed by lower density. The influence of the samples' height on the thermal runaway and the thermal gradient within the samples are discussed as responsible for these effects.

Keywords: grain growth, electrical properties, ceramics, 3YSZ, electric field-assisted sintering.

Flash sintering has gained wide attention since it was reported in 2010 [1] due to the benefits it can offer when compared with conventional sintering. By applying this technique, the sintering time is typically reduced by three orders of magnitude, changing from hours (conventional sintering) to just a few seconds (flash sintering). The furnace temperature required to sinter the material can also be substantially reduced, *e.g.*, 3YSZ was flash sintered at 850°C [1]; 8YSZ at 390°C [2]; $MnCo_2O_4$ at 120°C [3]. More remarkably, ZnO [4-5] and UO_2 were flash sintered at room temperature [6]. Reducing time and temperature during ceramic processing implies decreasing energy consumption and discarding the necessity of using robust furnaces.

Despite these advantages, flash sintering still has issues that make difficult to apply it on the industrial scale. Microstructural heterogeneity of flash sintered samples has been frequently reported [7-9]. For instance, Steil *et al.* [7] observed grain size differences between the core and the surface of flash sintered 8YSZ. Carvalho *et al.* [8] also verified microstructural heterogeneity and suggested that it could be related to inhomogeneities in the green ceramics after compacting, which might contribute to a current preferred path. Campos *et al.* [9] reported a significant difference between grain sizes at the vicinities of the cathode and the anode for pellets of 3YSZ flash sintered under a DC electric field. However, no microstructural heterogeneity was verified for 3YSZ, when using dog-bone shaped samples [1,10] and the same flash conditions as reported by Campos et al. [9]. This indicates that the geometry of the sample and the electrodes might play an important role in the heterogeneity observed.

In this work we investigate the effects of the height (h) of cylindrical samples on the microstructural characteristics and onset temperature of flash for 3YSZ.

Commercial powders of 3YSZ — TZ-3Y-E, Tosoh (average particle size of 40 nm and a specific surface area of 16 ± 3 m^2/g) were mixed with a binder solution following the procedure described in a previous work [9]. Cylindrical shaped samples were uniaxially pressed at 70 MPa and then isostatically pressed at 200 MPa. Pellets with 6 mm diameter and h = 2, 4, 6, 8, and 10 mm were produced. Three samples of each height were prepared.

The green ceramics were calcinated at 600°C for 1 h, with a heating rate of 5°C/min, for removing the organic binder. Thereafter, flash sintering was performed using a self-made automated setup [9]. The flash sintering parameters were: furnace heating rate of 20°C/min; maximum current density set to 100 mA/mm^2 (RMS basis); electric field of 90 V/cm (RMS basis) in AC (alternate current mode) with sinusoidal waveform at a frequency of 1 kHz. The voltage was applied to Pt disc electrode in contact with the flat surface of the samples. No conductive pastes were used between the disc electrodes and the samples. The discs were polished to improve electrical contact before each sintering. A load of 2 bar was applied to guarantee the contact between the electrodes and sample. The power supply was turned-on since the beginning of the heating ramp and then turned off after 60 seconds of the flash event (the moment when the current density achieved 100 mA/mm^2). After sintering, the final density of the ceramics was measured by the Archimedes principle.

Figure 1 presents the onset temperature of the flash event as well as the ceramic relative density as a function of h. We have considered the

onset of flash when the current density has reached 20% of their maximum value (20 mA/mm^2). It is possible to notice that the height of the sample significantly affects the onset temperature of the flash event, even using the same electrical field strength of 90 V/cm. By increasing *h* from 2 to 10 mm, the onset of the flash decreased from 1172 to 875 °C. Furthermore, the final density of the ceramics also decreased with *h*.

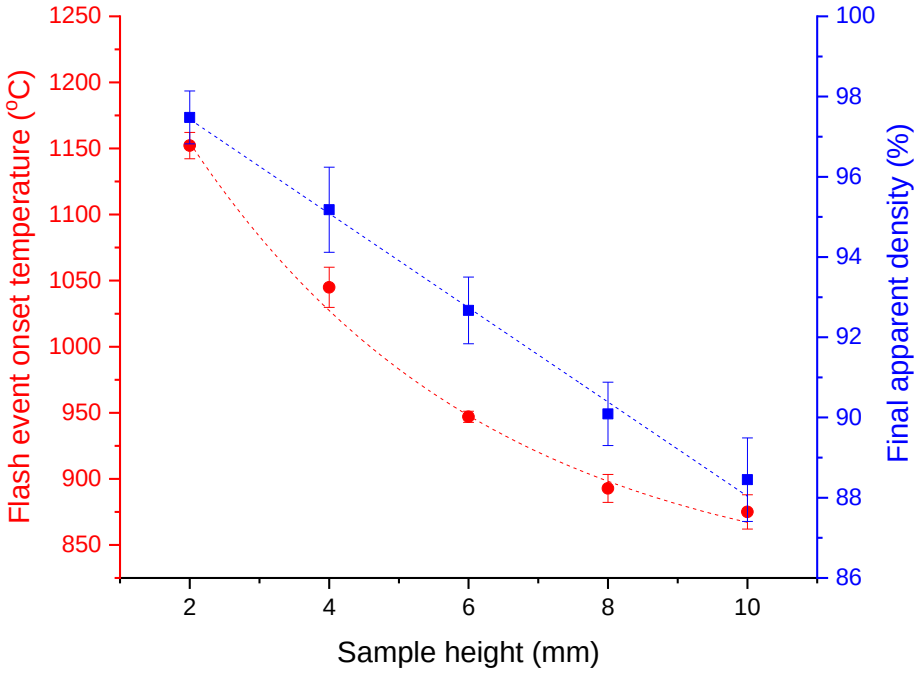

Figure 1. The plot of the onset temperature of the flash event and the final apparent density of flash sintered samples (measured by Archimedes principle) in the function of the cylindrical samples' height.

After flash sintering, the microstructure of the ceramics was analysed by scanning electron microscopy (SEM). The samples were cut in their radial center and then polished. Afterwards, thermal etching was performed at 1350 °C for 10 min, using a heating rate of 10 °C/min. Three regions of the polished surface were analysed for each ceramic: near the electrodes (10 –

20 µm from the cylinders flat surface), at the cylindric radial surface (10 – 20 µm from the radial surface), and at the core. These results are illustrated in Figure 2, which shows the micrographs from the samples with different heights at three different regions (core, 10 – 20 µm from the radial surface, and 10 – 20 µm from the flat surface). It is clearly seen that the smaller the samples were, the smaller were their grains. Besides that, bigger samples presented grain size heterogeneity between the regions (core presented bigger grains). Furthermore, we also observed cavitation for samples with h = 6, 8, and 10 mm height, which could justify their lower density (see Fig. 1) [11].

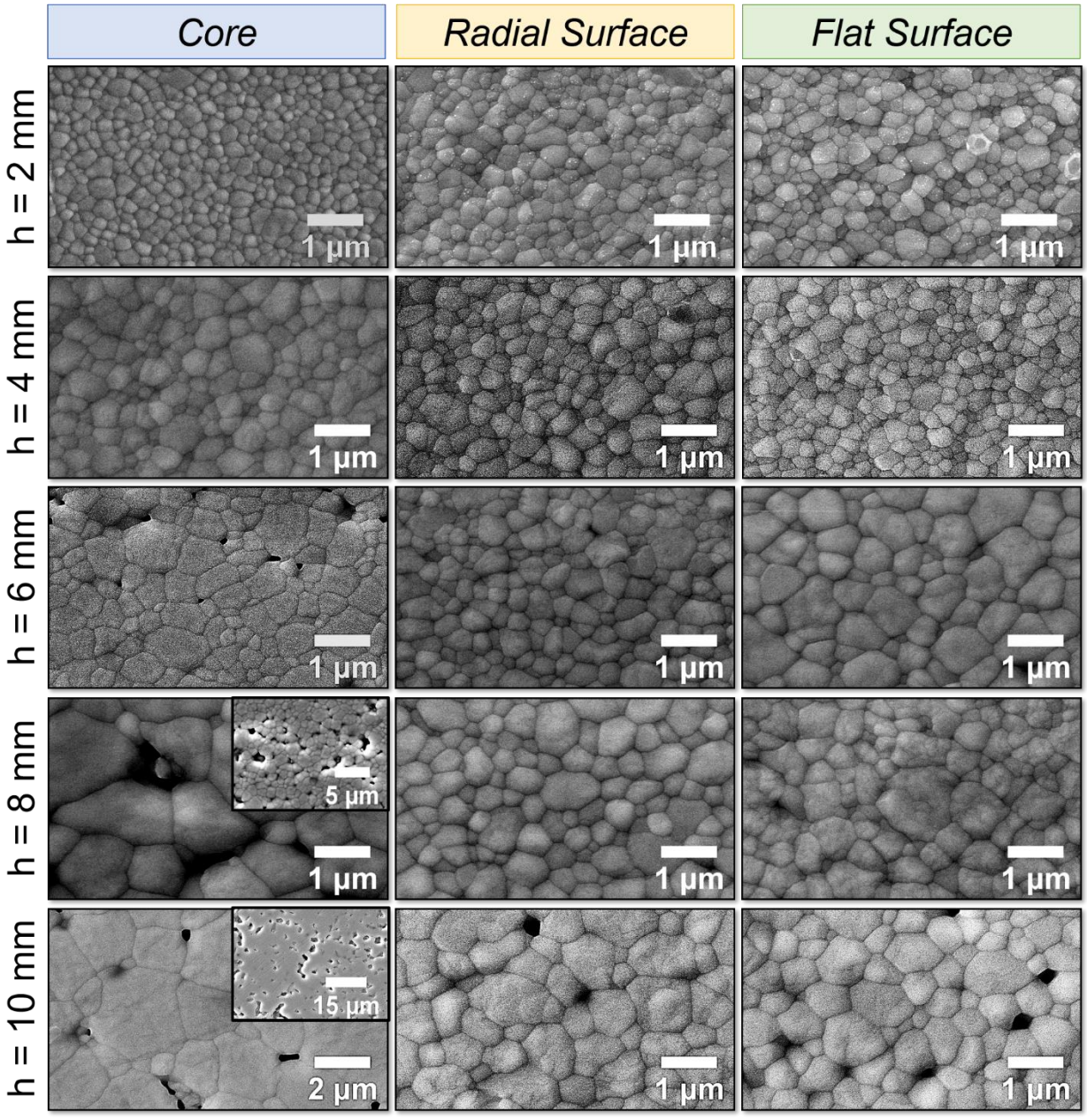

Figure 2. Micrographs of core, radial surface, and flat surface of samples with *h*= 2, 4, 6, 8, and 10 mm height; Note that the scale of the core's SEM image of the sample with 10 mm height is different from the others; Insets on the core micrographs of sample with *h*= 8 and 10 mm are micrographs with less magnification.

Grain size gradients were observed at the samples with *h*= 8 and 10 mm. For instance, the grain size of the core of the sample with *h*= 10mm was 3x bigger than its grain size near the open surface. The software Image J (National Institute of Health) was used to determine grain size distribution of the ceramics. Afterwards, the average grain size (AGS) from each of the five regions was compared using Tukey's test with 5% of significance. At least 200 grains were measured for each sample region. Table 1 summarizes the AGS at the different regions of the sample. The flat and radial surfaces were represented together in Table 1 since it has no significant difference from each other.

Table 1. Average grain size of the core, and the surfaces of the samples with 2, 4, 6, 8, and 10 mm height; Tukey test represents if the average grain size of the core and the surface were considered equal with a 5% significance; the "=" symbolizes that the core and the surfaces had an equal average grain size, and then the sample was considered homogeneous, and "≠" symbolizes the other way around

Sample height	Average grain size (μm)			Tukey (5%)
	Surfaces	Core	Mean	
2	0.18 ± 0.016	0.21 ± 0.015	0.19 ± 0.011	=
4	0.25 ± 0.020	0.53 ± 0.027	0.43 ± 0.018	=
6	0.43 ± 0.030	0.66 ± 0.024	0.58 ± 0.019	=
8	0.78 ± 0.037	1.22 ± 0.053	0.91 ± 0.048	≠
10	0.81 ± 0.037	2.43 ± 0.069	1.13 ± 0.052	≠

It would be expected the same onset temperature of the flash event for all the studied samples once in all the cases the same electric field was applied [1,9,11,12]. Besides different onset temperatures, larger grains

were observed when increasing *h* (Table 1). This larger AGS may indicate that taller samples were at higher sintered at a higher temperature. We attribute these observations due to thermal gradient during the flash sintering.

The difference in the grain size between the regions of the core and the surfaces (Figure 2 and Table 1) may be due to the kinetics of heat losses by conduction (near the electrode surface), and by radiation (at the open surface). Since the core would have more difficulty to dissipate the heat, it should be hotter than the other regions. This is mostly seen on thicker and larger samples since the distance between the core to the surfaces is bigger in those cases [7-10].

Besides that, the sample height could also influence the thermal runaway ignition. Considering the overall thermal runaway model for flash sintering, as already reported by Dong et al. [13] and other works [14-16], the sample temperature is determined by a heat balance between the power dissipated and the heat losses to the ambient, either by convection, conduction or radiation, as described in equation (3):

$$V\rho C_p \frac{dT}{dt} = P_{Joule} - L(T) \quad (1)$$

In the above ρ is the material density, C_p is the heat capacity, and L(T) is the heat losses to the environment. Using the approach developed by Pereira da Silva et al. [16], an effective convection coefficient (h_{eff}) can be determined to lump all the heat loss contributions to the furnace and the contributions to the cooling from the electrodes, and therefore facilitate an analytical solution to the thermal runaway problem:

$$\rho C_p \frac{dT}{dt} = \frac{E^2 e^{\frac{Q}{R_g T}}}{\sigma_0} - h_{eff}\frac{A_T}{V}(T - T_0) - 4k\frac{A_E}{hV}(T - T_0) \quad (2)$$

In the above A_T is the surface area of the sample, k the thermal conductivity of the heat sink, A_E is the area in contact with the electrodes, h is the sample height and T_0 is the furnace temperature. The conditions for thermal runaway are satisfied where a non-smooth transition in the folds of the equilibrium surface defined by $\frac{dT}{dt} = 0$ happens. By implicit differentiation as a function of the temperature of equation (4) when $\frac{dT}{dt} = 0$, and returning to equation (2), it is possible to determine the critical furnace temperature for thermal runaway as a function of the processing parameters:

$$T_0 \geq -\frac{Q}{R_g}\left\{\frac{1 + 2W\left[\frac{-1}{2E}\sqrt{\frac{\sigma_0 Q}{VR_g}\left(h_{eff}A_T + \frac{4kA_E}{h}\right)}\right]}{4W\left[\frac{-1}{2E}\sqrt{\frac{\sigma_0 Q}{VR_g}\left(h_{eff}A_T + \frac{4kA_E}{h}\right)}\right]^2}\right\} \quad (3)$$

In equation (3) W is the LambertW function.

The Figure 3 illustrate the lower and upper bound of the flash onset temperature in function of the sample's height predicted by the equation (3) model. It is evident that the equation (3) is coherent with the experimental data.

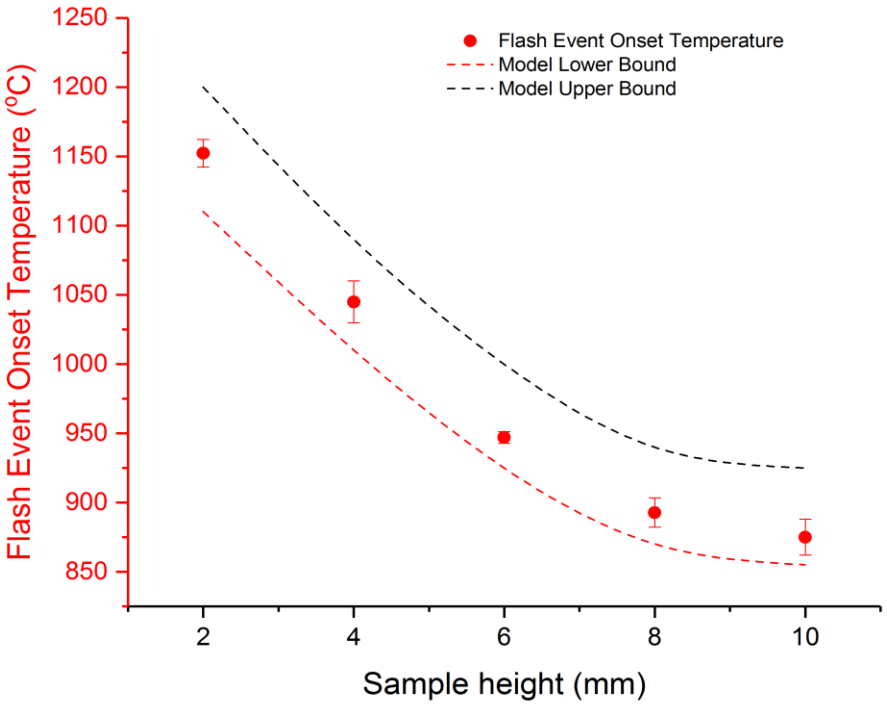

Figure 3. Flash onset temperatures predicted by equation (3) as a function of the sample height.

By analysing equations (2) and (3), it can be observed the heat sink effect of radiation/convection is the same for all the samples, since the ratio A_T/V is constant for cylindrical samples with increasing height. The higher difference is in the magnitude of the conduction term to the electrodes, and with taller samples, this heat loss is more pronounced, which can be observed not only on the model predictions but also in the higher degree of inhomogeneity observed, likely caused by the temperature differences between the core of the sample and the region in contact with the electrodes.

Figure 4 (a) shows the electric field behavior during the flash sintering experiments for all different sizes of samples. As bigger as the samples were, higher was the drop on electric field after the current control mode (third stage of flash sintering). It can be attributed to electrical current concentration at the core of taller samples, which can either explain the higher electric field drop on this samples and also their bigger gran size heterogeneity. Since we consider that is a thermal gradient at the taller samples, we might also consider an electrical conduction gradient.

Figure 4 (b) presents the rising of the current density during the flash sintering for different samples heights. It could be noticed that as bigger as the samples was, more abruptly the flash event happened. This behavior was already predicted by Pereira da Silva et al. with a bifurcation model. [17]

Figure 4 (c) shows the power density, which is higher for smaller samples. It was also observed that more abrupt transitions of flash increase the chance of power peak appearing. It also could be seen with the bifurcation model proposed by Pereira da Silva et al. [16] combined with the third stage conditions.

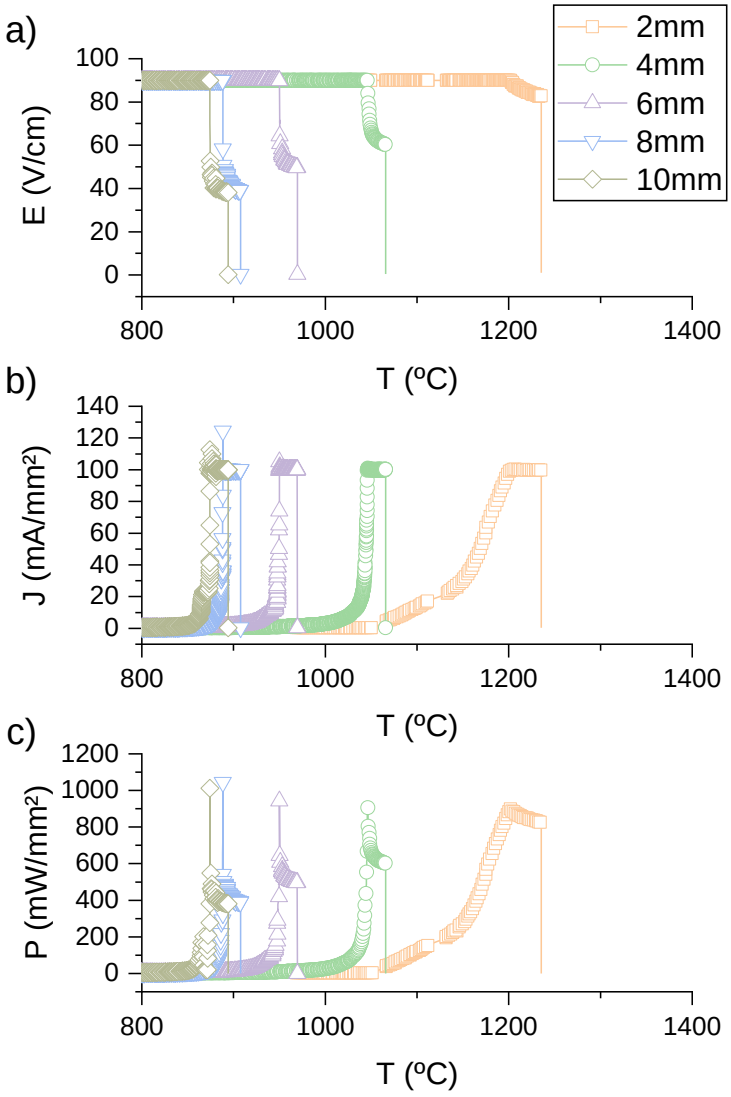

Figure 4. Plots of (a) Electric field - E, (b) current density - J, and (c) power density - P vs furnace temperature (T) of samples with different sizes during the flash sintering.

The electrical energy (Σ) used for each condition was calculated by integrating the power density over time. The energy of each condition was calculated during the onset and the steady-state of flash (the subscript refers to the samples height): Σ_{2mm}= 215.21 J·mm^{-3}, Σ_{4mm}= 53.39 J·mm^{-3}, Σ_{6mm}=

40.94 $J \cdot mm^{-3}$, Σ_{8mm}= 30.40 $J \cdot mm^{-3}$, Σ_{10mm}= 28.74 $J \cdot mm^{-3}$. We observed that as larger as the samples were, smaller were their energy. It happened because smaller samples presented a smoother rise in their electrical current. The influence of the geometry parameters, such as sample height, on the abruptness of the flash transition is in accordance with the dynamic bifurcation criterium presented by Pereira da Silva et al. [16].

In summary, it was observed that the cylindrical sample height exerted a significant influence on flash onset temperature, final apparent density, and microstructure (grain size and homogeneity). This has been suggested to occur due to two possible reasons or even a combination of them: (1) sample's height is an important parameter for initiating the thermal runaway and then the flash event; and (2) the thermal gradient and consequently the local electrical conductivity gradient.

Thus, samples with different geometries may present different results under the same flash sintering conditions and therefore the geometric characteristics should be taken into account when comparing samples obtained by this technique, or when scaling up the flash sintering for use on an industrial scale.

Acknowledgments

Funding: This work was supported by the São Paulo State Research Support Foundation (FAPESP) [2015/07319-8, and 2018/04331-5], and the Coordination for the Improvement of Higher Education Personnel - Brazil (CAPES) [001].

The authors thanks Lilian M. Jesus for valuable help reviewing this work.

References

[1] M. Cologna, B. Rashkova, R. Raj, J. Am. Ceram. Soc., 93 (2010), n. 11, pp. 3556–3559.

[2] J.A. Downs, V.M. Sglavo, J. Am. Ceram. Soc., 96 (2013), n. 5, pp.1342–1344.

[3] A. Gaur, V.M. Sglavo, J. Eur. Ceram. Soc., 34 (2014), pp. 2391–2400.

[4] J. Nie, Y. Zhang, J.M. Chan, R. Huang, J. Luo, Scr. Mater., 142 (2018), pp. 79–82.

[5] J. Liu, X. Li, X. Wang, R. Huang, Z. Jia, Scr. Mater., 176 (2020), pp. 28-31.

[6] A.M. Raftery, J.G. Pereira da Silva, D.D. Byler, D.A. Andersson, B.P. Uberuaga, C.R. Stanek, K.J. McClellan, J. Nucl. Mater., 493 (2017), pp. 264–270.

[7] M.C. Steil, D. Marinha, Y. Aman, R.C.J. Gomes, M. Kleitz, J. Eur. Ceram. Soc., 33 (2013), n. 11, pp. 2093–2101.

[8] S. Carvalho, E. Muccillo, R. Muccillo, Ceram., 1 (2018), n. 2, pp. 1–10.

[9] J.V. Campos, I.R. Lavagnini, R.V. Sousa, J.A. Ferreira, E.M.J.A. Pallone, J. Eur. Ceram. Soc., 39 (2019), n. 2-3, pp. 531–538.

[10] M.K. Punith Kumar, D. Yadav, J.M. Lebrun, R. Raj, J. Am. Ceram. Soc., 102 (2019), n. 2, pp.823-835.

[11] Y. Dong, I. Chen, J. Am. Ceram. Soc., 101 (2018), n.3, pp.1058-1073.

[12] J.S.C Francis, R. Raj, J. Am. Ceram. Soc., 96 (2013), n. 9, pp. 2754-2758.

[13] Y. Dong, W. Chen, J. Am. Ceram. Soc., 98 (2015), n.12, pp.3624-3627.

[14] I.J. Hewitt, A.A. Lacey, R.I Todd, Math. Model. Nat. Phenom., 10 (2015), n. 6, pp. 77-89.

[15] R.I. Todd, E. Zapata-Solvas, R.S. Bonilla, T. Sneddon, P.R. Wilshaw, J. Eur. Ceram. Soc., 35 (2015), n.6, pp.1865-1877.

[16] J.G. Pereira da Silva, H.A. Al-Qureshi, F. Keil, R. Janssen, J. Eur. Ceram. Soc., 36 (2016), n. 5, pp.1261-1267.